Metabolic-activity based assessment of antimicrobial effects by D2O-labeled Single-Cell Raman Microspectroscopy

Journal:	*Analytical Chemistry*
Manuscript ID	ac-2016-05051v.R1
Manuscript Type:	Article
Date Submitted by the Author:	28-Feb-2017
Complete List of Authors:	Tao, Yifan; Sun Yat-sen University, Department of Operative Dentistry and Endodontics; Chinese Academy of Sciences, Qingdao Institute of BioEnergy and Bioprocess Technology Wang, Yun; Chinese Academy of Sciences, Qingdao Institute of BioEnergy and Bioprocess Technology Huang, Shi; Chinese Academy of Sciences, Qingdao Institute of BioEnergy and Bioprocess Technology Zhu, Pengfei; Chinese Academy of Sciences, Qingdao Institute of BioEnergy and Bioprocess Technology Huang, Wei; University of Oxford, Department of Engineering Science Ling, Jun-Qi; Guanghua School of Stomatology Xu, Jian; Chinese Academy of Sciences, Qingdao Institute of BioEnergy and Bioprocess Technology

Metabolic-activity based assessment of antimicrobial effects by D_2O-labeled Single-Cell Raman Microspectroscopy

*Yifan Tao[1,2], Yun Wang[2,4], Shi Huang[2,4], Pengfei Zhu[2,4], Wei E Huang[3], Junqi Ling[1,] *, Jian Xu[2,4,] **

[1]Operative Dentistry and Endodontics, Guanghua School of Stomatology, Affiliated Stomatological Hospital, Guangdong Province Key Laboratory of Stomatology, Sun Yat-Sen University, Guangzhou, Guangdong, 510055, China

[2]Single-Cell Center, CAS Key Laboratory of Biofuels and Shandong Key Laboratory of Energy Genetics, Qingdao Institute of BioEnergy and Bioprocess Technology, Chinese Academy of Sciences, Qingdao, Shandong, 266101, China.

[3]Department of Engineering Science, University of Oxford, Parks Road, Oxford, OX1 3PJ, United Kingdom.

[4]Univesity of Chinese Academy of Sciences, Beijing, 100049, China.

*Corresponding author: Jian Xu and Junqi Ling

xujian@qibebt.ac.cn and lingjq@mail.sysu.edu.cn

Telephone:+86 (0)532-80662651

ABSTRACT

To combat the spread of antibiotic resistance, methods that quantitatively assess metabolism-inhibiting effects of drugs in a rapid and culture-independent manner are urgently needed. Here using four oral bacteria as models, we show that heavy water (D_2O) based Single-cell Raman Microspectroscopy (D_2O-Raman) can probe bacterial response to different drugs using the Raman shift at C-D (carbon-deuterium vibration) band in 2,040 to 2,300 cm^{-1} as a universal biomarker for metabolic activity at single bacterial cell resolution. "Minimum Inhibitory Concentration based on Metabolic Activity" (MIC-MA), defined as the minimal dose under which the median ΔC-D-ratio at 8 h of drug exposure is ≤0 and the Standard Deviation (SD) of the ΔC-D ratio among individual cells is ≤0.005, was proposed to evaluate the metabolism-inhibiting efficacy of drugs. In addition, Heterogeneity Index of MIC-MA (MIC-MA-HI), defined as SD of C-D ratio among individual cells, quantitatively assesses the among-cell heterogeneity of metabolic activity after drug regimens. When exposed to 1× MIC of sodium fluoride (NaF), 1× MIC of chlorhexidine (CHX) or 60× MIC of ampicillin, the cariogenic oral pathogen *Streptococcus mutans* UA159 ceased propagation yet remained metabolically highly active. This underscores the advantage of MIC-MA over the growth-based MIC in being able to detect the 'non-growing but metabolically active' (NGMA) cells that underlie many latent or recurring infections. Moreover, antibiotic susceptible and resistant *S. mutans* strains can be readily discriminated at as early as 0.5 h. Thus D_2O-Raman can serve as a universal method for rapid and quantitative assessment of antimicrobial effects based on general metabolic activity at single-cell resolution.

Introduction

To combat the rapid spread of microbial drug resistance, fast, sensitive and reliable methods for quantitative assessment of antimicrobial activities are urgently needed[1-2]. Currently such methods can be broadly classified as 'growth-based' or 'non-growth based'. Growth-based methods typically examine the sensitivity of cell growth curve to drugs via dilution and diffusion, and quantitative parameters such as 'minimum inhibitory concentration' (MIC) was derived[3]. These methods can be time consuming (frequently exceeding 24 h for the most common pathogens as extended duration of drug exposure is required), and moreover are usually not capable of tackling viable but nonculturable microbes[4-5]. Furthermore, as growth inhibition does not necessarily correlate with metabolic inhibition or cell death, growth-based methods are usually not capable of distinguishing between bactericidal and bacteriostatic effects and consequentially fail to detect 'non-growing but metabolically active' (NGMA) cells, which are responsible for many latent or recurring infections (due to their ability to resume growth after removal of antimicrobials) and eventually lead to treatment failure[6].

On the other hand, non-growth based approaches measure cellular phenotypes that correlate with inhibition of cellular metabolism, independent of cell proliferation[7-8]. For example, intracellular ATP content of a cellular population, which is typically reduced due to drug inhibition of cellular metabolism, can be assayed via luminescence generated by luciferase-catalyzed luciferin oxygenation that uses ATP as energy supply[9]. However, despite their value in assessing the drug effect on energy metabolism, such methods can be misleading when the drug targets other cellular processes or even elevates intracellular ATP level (e.g., in the case of rifampin, as a response to respiration-deceleration[10]). Moreover, ATP assays, normally performed at the bulk cell level, measure ensemble-averaged parameters and are unable to assess the heterogeneity of drug sensitivity or drug response within a microbial population or a consortia[11]. Recently, to probe the impact of antibiotics on energy metabolism at single-cell resolution, a genetically encoded FRET (Förster resonance energy transfer pair) of cyan and yellow fluorescent proteins flanking the epsilon subunit of the *Bacillus subtilis* F_oF_1 ATP synthase was genetically introduced into *Mycobacterium smegmatis* as a sensor of intracellular ATP level[12]. However, the prerequisite for genetic manipulation (i.e., introduction of the reporter gene) limits the types of cells applicable, and essentially precludes its application on non-model organisms, uncultivated microbes, *in situ* analysis or point-of-care diagnosis.

Single-cell Raman Microspectroscopy is a non-destructive and externally label-free approach that provides comprehensive intrinsic molecular profile based on the vibrational frequencies of characteristic chemical bonds in a cell. Single-cell Raman Spectra (SCRS) have been employed to monitor bacterial phenotypic changes, mostly of macromolecule contents inside cells, during antimicrobial treatment at

either the population or the single cell level[13-15]. Recently we proposed the 'Ramanome' concept, and showed that a combination of 31 specific Raman peaks (i.e., Raman Barcode of Cellular Stress-response or RBCS) from SCRS randomly sampled from a cellular population can discriminate drug response programs based on cytotoxicity mechanism[15]. However, the multivariate nature of Ramanome, as well as its sensitivity to each of genetic background, physiological state and environment changes, can confound quantitative modeling and cross-species comparison of drug response.

In the presence of heavy water D_2O, electron carriers NADPH and NADH, which are associated with cell general metabolic activity, can exchange H^+ in $NADPH+H^+$ with D^+ from D_2O, and incorporate D^+ to form C-D bonds[16-17]. In D_2O based Single-cell Raman microscopy (D_2O-Raman), the rate of deuterium uptake in individual live cells via NADPH/NADH can be modeled by tracking the temporal shifting of C-H band to C-D band in a SCRS, due to the graduate substitution of C-H by the C-D bonds in intracellular macromolecules such as lipids and carbohydrates [16-19]. As intake of H_2O or D_2O is a universal and basic property of living cells, we hypothesize that D_2O-Raman can serve as a non-invasive, quantitative and universal method to detect and measure metabolic activity of cells in response to drug treatments. "Minimum Inhibitory Concentration based on Metabolic Activity" (MIC-MA) was proposed to evaluate metabolism-inhibiting efficacy of drugs. In addition, Heterogeneity Index of MIC-MA (MIC-MA-HI), defined as Standard Deviation (SD) in C-D ratios of individual cells, was employed to quantitatively assess the heterogeneity of cellular metabolic activity in an isogenic population responding to drug regimens. We further showed that the method is able to detect the NGMA cells. Moreover, D_2O-Raman can rapidly discriminate between antibiotic susceptible and resistant *S. mutans* strains. Thus D_2O-Raman represents a universal method for rapid and quantitative assessment of antimicrobial effects based on metabolic activity at the single-cell level.

Experimental methods

Microorganisms and growth conditions

Five oral bacteria were tested in this study: (1) *Streptococcus mutans* UA159, (2) the fluoride-resistant *Streptococcus mutans* C180-2FR[20], (3) *Streptococcus gordonii* ATCC10558, (4) *Streptococcus sanguinis* ATCC10556, and (5) *Lactobacillus fermentum* ATCC9338. Details of growth conditions, D_2O exposure and drug administration are provided in **Supporting Information**.

Acquisition and analysis of Single-cell Raman spectrum

Cell pretreatment and SCRS acquisition were performed using a modified Raman spectrometer as described previously[15, 17]. All SCRS were processed by background subtraction (background defined as

the spectra of cell-free regions on the same slide), baseline correction and normalization using the Labspec5 software (Horiba Jobin Yvon Ltd, UK). The band intensity was normalized against (*i*) the total area of the Raman spectrum or (*ii*) intensity of the tallest band in the Raman spectrum. The latter was chosen in this work as the two normalization methods yield identical values of the 'C-D ratio'. The C-D ratio was defined as percentage of the integrated spectral intensity of the C-D band (2,040-2,300 cm^{-1}) as compared to the sum of the C-D band and the predominant C-H band (2,800-3,100 cm^{-1}), so as to quantify the degree of D substitution in C-H bonds. Standard deviation (SD) of the C-D ratio of individual cells was used to quantify the degree of heterogeneity in D substitution. Chemometrics analyses were performed using R (version 3.3.1) via customized scripts. Additional details are provided in **Supporting Information**.

Results and Discussion

Tracking deuterium incorporation in oral bacteria via Single-Cell Raman Spectra

Oral microbiota play key roles in not only oral infections but also systemic diseases[21-24]. Here employing four prevalent members of oral microbiota that include the Gram-positive *Streptococcus mutans* (strain UA159), *Streptococcus gordonii* (strain ATCC10558), *Streptococcus sanguinis* (strain ATCC10556) and the Gram-negative *Lactobacillus fermentum* (strain ATCC9338), we tested the general applicability of the D_2O-Raman method in assessing bacterial metabolic activity. We started by probing the sensitivity of bacterial growth to the D_2O level in the medium. Compared with the control (i.e., D_2O-free conditions) and as measured by OD_{600} (**Supporting Information**), D_2O of ≤ 40% in the medium did not have significant inhibition on growth of *S. mutans* UA159 and *S. sanguinis* ATCC10556 (**Fig. S1**), whereas *S. gordonii* ATCC10558 was more sensitive to D_2O. Interestingly, among these four model strains, *L. fermentum* ATCC9338 was able to tolerate high levels of D_2O (up to 50%) (**Fig. S1**).

For each of the bacteria and at each of the D_2O levels tested, a broad C-D Raman band in 2,040 to 2,300 cm^{-1} region emerged in SCRS, which was caused by a Raman shift of the original C-H peak (between 2,800 and 3,100 cm^{-1})[16] and intensity of the C-D band is proportional to D_2O level in the medium (**Fig. S2**), suggesting that all of these four bacteria actively take in D_2O. No visible C-D peak was observed in D_2O-free cultures and the 2,040 to 2,300 cm^{-1} region was flat as a 'silent zone' (**Fig. S2**). Moreover, emergence of the C-D peak was rapid and does not require cell replication: e.g., in *S. mutans* (doubling time of 60 ± 5.5 min[25]), the C-D band was detected at as early as 30 mins under 30% D_2O (**Fig. S3A**). In fact, temporal dynamics of the C-D band were different from the bacterial OD based

growth curve (**Fig. S3B**), since the C-D band appeared almost instantaneously after addition of D_2O and reached the 'logarithmic' phase ~3 h earlier than the growth curve.

On the other hand, temporal increase of the C-D ratio eventually reached a plateau during the first 8 h for *S. mutans* (**Fig. S3B**). Such "maximal C-D ratios" (defined as the C-D ratio at the plateau in the absence of drugs) were linearly correlated with D_2O level in the medium, although their slopes varied (with *S. sanguinis* being the highest and *L. fermentum* the lowest; **Fig. 1**). Under 30% D_2O, for each of the bacteria tested, the dynamic range of the C-D band was significant to allow quantification of its intensity change, while bacterial growth remained unaffected (largely equivalent to that under deuterium-free medium), hence 30% D_2O was chosen as the default level in the medium for modeling single-cell metabolic rates under various types, doses and exposure durations of drugs.

Kinetics of the C-D ratio quantitatively models metabolic inhibition of *S. mutans* UA159 by three antimicrobials

S. mutans UA159 is a clinical cariogenic strain that converts dietary carbohydrates to acids which can eventually result in tooth demineralization[26]. To model its drug sensitivity, two antiseptics (NaF and CHX) and one antibiotic (ampicillin), which are active ingredients in the mouthwash and frequently used antibiotics for treating oral infections respectively, were chosen as models here to test the cellular response to drugs. Traditional methods for drug efficacy evaluation are mostly based on MIC, defined as the minimal dose under which no visible bacterial growth (e.g., as measured by OD_{600}) was detected over 24 h of drug exposure (**Supporting Information**). The MICs of NaF, CHX and ampicillin for *S. mutans* UA159 and that of NaF for *S. mutans* C180-2FR were first measured via OD_{600}-based growth inhibition (**Table S1**). Then D_2O-Raman based *S. mutans* UA159 responses were examined under various doses for each drug. Temporal dynamics of the C-D ratio under NaF (**Fig. 2A**), CHX (**Fig. 2B**) and ampicillin (**Fig. 2C**) treatment for up to 8 h shared several features. (*i*) These curves consist of a 'lag' phase (e.g., under >MIC levels of NaF or CHX; the corresponding C-D ratio was termed as the 'baseline C-D ratio'), followed by a 'logarithmic' phase and then eventually a 'saturated' phase (the corresponding C-D ratio was termed as the 'saturated C-D ratio' for that particular dose). In the absence of drugs, only the latter two phases were present and the saturated C-D ratio became the 'maximal C-D ratio', which is a characteristic value to a given type of cells. (*ii*) Cells were highly sensitive to drug doses, as increasing drug doses led to extension of the 'lag' phase, lower level of 'logarithmic' phase and reduced 'saturated C-D ratio'. In fact, the slope at the logarithmic phase reduced in response to increased drug doses, suggesting stronger inhibition of metabolic activity by higher drug doses. (*iii*) For each of the drugs, cellular response was rapidly detected by the C-D ratio even under the lowest doses; for example, under 0.2 g/L NaF (0.5× MIC) or 1.2 mg/L CHX (0.6× MIC), the difference to the drug-

free control can be detected as early as 0.5 h (p<0.01, Wilcoxon rank sum test; **Table S2**), suggesting high sensitivity of D_2O-Raman in detecting drug effect.

The time-course of the C-D ratio exhibited reproducible and highly distinct dose-dependency to the three drugs. For NaF (**Fig. 2A**), at 0.5× MIC (0.2 g/L), increase of the C-D ratio was initially lower than the drug-free control but reached nearly the same level as the control at 8 h. At the MIC dose of NaF (0.4 g/L), a 'lag' phase lasted 2 h, followed by a 4 h-long 'logarithmic' phase and then a 'saturated' phase with ~40% of the maximal C-D ratio. At doses 1.5× or 3× MIC (i.e., 0.6 g/L or 1.2 g/L) of NaF, the C-D ratio remained at the baseline level from the start, indicating a complete inhibition of metabolism under these two doses. For CHX (**Fig. 2B**), at 0.6× MIC (1.2 mg/L), increase of the C-D ratio was also greatly delayed and at 8 h reached the plateau at 84% of the maximal C-D ratio. Under MIC (2 mg/L), the C-D ratio increased in the first 2~3 h and then plateaued at only 35% of the 'maximal C-D ratio' at 8h, suggesting 65% reduced yet still active cellular metabolism. At 2× MIC (4 mg/L), the C-D ratio remained at the 'baseline C-D ratio' for the whole 8 h period, indicating completely inhibited cellular metabolism during the entire duration of CHX exposure.

In contrast, when cells were exposed to ampicillin in the range of 0 to the exceedingly high >60× MIC (50 mg/L), no 'lag' phases were present, and in each case, the C-D ratio rapidly reached 'saturated' phase (i.e., all before 3 h) at a very high 'saturated C-D ratio'(**Fig. 2C**). For example, after MIC-dose (0.8 mg/L) exposure for 8 h, a saturated C-D ratio was as high as 83% of the maximal C-D ratio. At the extreme high dose of >60× MIC (50 mg/L), the 'saturated C-D ratio' still remained 51% that of the maximal C-D ratio, indicating the presence of rather strong cellular metabolic activity after such treatments although cell growth was completely inhibited under 1× MIC (0.8 mg/L) of ampicillin (**Table S1**). This is drastically different to the dose response of NaF or CHX, as exposure to 2~3× MIC of NaF or CHX for just 30 min would have already brought the bacteria to the baseline of C-D ratio. Thus we hypothesized that under high dose of ampicillin, a large fraction of *S. mutans* cells would enter the NGMA state, where cells, despite not replicating, remain alive and retain a high level of metabolic activity.

To test this hypothesis, *S. mutans* UA159 were exposed to 50 mg/L ampicillin (~60× MIC), 1.2 g/L NaF (3× MIC) or 4 mg/L CHX (2× MIC) for 1.5 h in D_2O-free BHI first, centrifuged to remove residual medium and then transferred to fresh BHI supplemented with identical type and dose of the pretreated drug and 30% D_2O. The immediate detection by Single-cell Raman Microscopy revealed that the C-D ratio of SCRS from cells exposed to ampicillin increased within 1 h, while those exposed to NaF or CHX remained at the baseline C-D ratio (**Fig. S4**). To measure the degree of residual metabolic activity and thus quantitatively compare drug efficacy, ΔC-D-ratio was defined as difference of the C-D

ratio of individual cells between a time point and the average C-D ratio of cells at 0 h (i.e., the 'baseline C-D ratio') under a particular dose for a given drug. At 1 h, ΔC-D-ratio for ampicillin reached 0.0078±0.0007, much higher than the background values for NaF (0.0009±0.0007) and CHX (0.0002±0.0006; **Fig. S4**). Thus metabolic activity of the cells remained high after the pre-exposure to >60× MIC of ampicillin for 1.5 h, despite being fully inhibited by 3× MIC of NaF or 2× MIC of CHX in the same period, suggesting that a large fraction of *S. mutans* cells has entered the NGMA state specifically under 60× MIC of ampicillin.

To examine whether the treatment under high doses of the three drugs caused cell death or simply suppression of metabolic activity, *S. mutans* UA159 culture was sampled at various durations of drug exposure, washed to remove drug residuals and plated onto drug-free BHI agar. The Colony Forming Unit (CFU) was then measured to assess the post-drug-treatment cell viability. For NaF and CHX, the time-course pattern of CFU count was in agreement with that of the 'saturated C-D ratio', in that higher drug doses resulted in both lower CFU and lower 'saturated C-D ratio' (**Fig. 3**). However, for ampicillin, there was no such correlation between drug dose and CFU; moreover, even under 60× MIC, 8 h of ampicillin exposure did not eradicate all bacteria (1.96×10^7 CFU/mL, versus 6.90×10^6 CFU/mL for 3× MIC NaF and 7.70×10^5 CFU/mL for 2× MIC CHX respectively; **Fig. 3 inset**) but the CFU was lower than that for the control at 8 h (7.07×10^8 CFU/mL). Thus all three drugs are bactericidal, although the killing effect of ampicillin is much weaker than NaF or CHX.

Intracellular ATP level of a cell population can be an indicator of the efficacy of antimicrobial agents, as its fluctuation is a secondary effect of drug response[27]. Thus to further validate our C-D ratio based method, the results were further compared to the intracellular ATP level of cell populations under drug treatment (**Methods**). For *S. mutans* UA159 cultures, under a series of NaF or CHX doses, similar dynamic patterns were observed between the intracellular ATP content (**Fig. 4A, 4B**) and the C-D ratio (**Fig. 2A, 2B**). Basically, increase in drug doses resulted in the decrease of intracellular ATP content, similar to that for the C-D ratio. For *S. mutans* UA159 cultures under ampicillin, the dose response of the intracellular ATP content were different, and there was no correlation between the intracellular ATP content and ampicillin dose (**Fig. 4C**). Moreover, even under very high ampicillin doses such as ~60× MIC (50 mg/L), no significant reduction of ATP homeostasis was observed for the bacterial population (**Fig. 4C**).

These observations can be potentially explained by the distinct antimicrobial action modes of the three drugs. CHX and NaF are both antiseptics: NaF inhibits cellular enolase and membrane ATPases[28], while CHX disturbs the arrangement and integrity of the phospholipid bilayer of cells and causes inhibition of both membrane-bound and soluble ATPases[29], thus both drugs resulted in reduced ATP

yield[28-29]. On the other hand, ampicillin, a β-lactam antibiotic, irreversibly inhibits the transpeptidase required for cell wall synthesis during binary fission[30-32] and does not directly inhibit ATP homeostasis, and cells become longer without proper division[15]. This may explain the intracellular ATP content and the emergence of NGMA *S. mutans* cells after ampicillin treatment. Moreover, bactericidal antibiotics like ampicillin was thought to be of 'biphasic killing', in that an initial, rapid drop in bacterial counts represents the death of the majority, while a subsequent, much slower phase of action exerts poor killing effect of NGMA or persistence cells[33], which are consistent with the cell viability test here.

MIC-MA proposed for metabolic activity-based assessment of antimicrobial efficacy

To quantitatively model antimicrobial effects, the ΔC-D-ratio in SCRS at 8 h was chosen as the default parameter for assessing drug effect, as after 8 h of drug treatment the C-D ratio already plateaued and was essentially identical to that after 24 h-exposure (**Fig. S5**). Moreover, the area where ΔC-D-ratio is below zero (i.e., with no metabolic activity detected) was designated as 'metabolism quiescence zone' (**Fig. 5**). For NaF (**Fig. 5A**), CHX (**Fig. 5B**) and ampicillin (**Fig. 5C**), the averaged ΔC-D-ratios at 8 h were inversely proportional to the dose, despite a high degree of heterogeneity in ΔC-D-ratio among cells at each of the doses. Notably, for NaF and CHX, majority of the cells have entered the 'metabolism quiescence zone' under 2~3× MIC (1.2 g/L of NaF and 4 mg/L of CHX), which is different from ampicillin where none of the cells sampled entered the zone even under 60× MIC (50 mg/L).

Thus to quantify antibacterial efficacy via metabolism inhibition instead of growth suppression, "Minimum Inhibitory Concentration based on Metabolic Activity" (MIC-MA) was proposed, which was defined as the minimal dose under which the median value of ΔC-D-ratio at 8 h of drug exposure is ≤0 and the SD among the individual cells is ≤0.005. For *S. mutans* UA159, the MIC-MA of NaF and CHX was 1.2 g/L (300% of MIC) and 4 mg/L (200% of MIC) respectively (**Table 1**). However, no MIC-MA was found for ampicillin, as *S. mutans* UA159 is able to maintain a high level of metabolism even under 60× MIC of ampicillin (50 mg/L; **Fig. 5C**). For all the three drugs, MIC-MAs are higher than MIC (**Table 1**), which is expected as suppression of bacterial growth does not necessarily lead to inhibition of metabolic activity.

Moreover, a second parameter called Heterogeneity Index of MIC-MA (MIC-MA-HI), defined as Standard Deviation (SD) in C-D ratios of individual cells sampled from a given population, was proposed to quantitatively assess and track the heterogeneity of microbial metabolic activity under a particular time, dose and type of drug within a population; such heterogeneity in drug sensitivity is crucial in development of drug resistance[34] and thus should be of great value to evaluation of drug efficacy. For each of the three drugs and at every dose tested, the MIC-MA-HI was significant, ranging

from 0.002 at 1.2 g/L NaF and 0.011 at 1.2 mg/L CHX (**Fig. 5A, 5B**), underscoring the universality of microbial heterogeneity in drug response. For both NaF (**Fig. S6A**) and CHX (**Fig. S6B**), MIC-MA-HI was inversely proportional to drug dose. Higher doses generally resulted in lower heterogeneity along the 8 h of drug exposure, indicating that strong inhibition reduces heterogeneity of the metabolic activity across the population. Interestingly, for ampicillin (**Fig. S6C**), no inverse proportional correlation was observed (p>0.05, Kruskal-Wallis test). Clearly, information such as MIC-MA-HI can be of vital value in decision making for the recommended drug, dosage and duration of exposure, since after drug treatment a bacterial population or consortium that exhibits low average metabolic activity yet harbors a subpopulation with robust metabolism can lead to chronic or reoccurring infections[12].

The heterogeneity of metabolic activity at single cell resolution can also be measured by introducing into the cell a sensor (coupled to fluorescence) of intracellular ATP level [12]; however the prerequisite for genetic manipulation limits the application of such approaches to laboratory model organisms. In contrast, due to its label-free nature, the D_2O-Raman method may be generally applicable to most or all types of cells, and thus should be of particular value to non-model organisms, uncultivated microbes, *in situ* analysis and point-of-care diagnosis, where genetic transformation is typically not feasible or not readily available.

The D_2O-Raman Method distinguishes between drug susceptible and resistant *S. mutans*

Fluoride is a widely used anti-caries ingredient in drinking water, toothpaste and mouthwash[35], however fluoride-resistant *S. mutans* have emerged, causing failure or flawed control of tooth decay by fluoride[20]. To test whether our method can rapidly distinguish drug resistant strains, dynamics of the C-D ratio from SCRS was compared between the fluoride-sensitive (*S. mutans* UA159) and fluoride-resistant (*S. mutans* C180-2FR) strains under various doses of NaF. In the absence of fluoride (**Fig. 6A**), C-D ratios of the fluoride-resistant strain were lower than those of the sensitive strain in the first 3 h of inoculation and then reached a similar level after 4 h. This can be explained by the longer doubling time of C180-2FR (74.5 ± 13.2 min)[36] than UA159 (60 ± 5.5 min)[25]. Under 0.4 g/L NaF (MIC for UA159), for the fluoride-sensitive strain the C-D ratio stayed in the 'lag' phase before 2 h and then increased rapidly thereafter. In contrast, for the fluoride-resistant strain, the temporal pattern of the C-D ratio was identical to that under NaF-free medium, suggesting that its metabolic activity was unaffected and the strain was insensitive to 0.4 g/L NaF (**Fig. 6B**). In fact, the C-D ratio is able to distinguish the two strains in as early as 0.5 h (p<0.01, Wilcoxon rank sum test; **Table S3**). Under 1.6 g/L NaF (MIC for C180-2FR) for the resistant strain or under 1.2 g/L NaF (3× MIC for UA159) for the sensitive strain, although cell metabolism (as measured by the C-D ratio) were consistently weaker at each time point than under NaF-free and 0.4 g/L NaF conditions, the C-D ratio of fluoride-sensitive strain remained at

the baseline level throughout the 8 hrs, yet in contrast, that of the resistant strain started increasing rather rapidly after 1 h (**Fig. 6C**). Thus D_2O-Raman is able to rapidly screen drug-resistant microbes.

Conclusions

The spread of drug resistance demands rapid, sensitive and reliable methods for quantitative assessment of antimicrobial activities[1-2]. Here we developed the D_2O-Raman method as a growth-independent approach for measurement of cellular metabolic activity in response to drug treatment at the single-cell level. In addition, MIC-MA was proposed as a basis for quantitative assessment and comparison of drug efficacy based on residual metabolic activity of the bacteria as well as the associated intercellular heterogeneity quantified by MIC-MA-HI.

The D_2O-Raman method, which can be considered as one extreme case of the Ramanome approach[15], has several advantages compared to other single-cell phenotyping methods. (*i*) It allowed measurement of metabolic activity of individual cells without prior knowledge of their physiology status or changing their biological context. (*ii*) D_2O can be directly combined with any external stimuli to probe their effects on target cells. (*iii*) D_2O uptake is more sensitive and rapid than other stable isotopes such as ^{13}C in inducing detectable change in SCRS[17]. (*iv*) In the presence of D_2O, dead cells are unable to form C-D bands in SCRS, which can be readily distinguished from those NGMA cells. (*v*) Due to its non-destructive manner, this method can be coupled to Raman-activated Cell Sorting and the subsequent single-cell DNA/RNA sequencing[37-42], thus linking bacterial genotypes to key phenotypes such as those underlying antibiotic-resistant or dormant sub-populations in recurrent infections[5,6]. On the other hand, the D_2O-Raman method can be labor-intensive and of low throughput. As the Raman spectrum for each bacterial cell took 10 seconds to acquire and at least 20 cells were randomly selected manually for imaging, currently it can take 5~10 mins for analyzing each cell population. Ongoing software development in our laboratory that automates cell selection, SCRS acquisition and data analysis should greatly improve the throughput of D_2O-Raman experiments.

Finally, although several oral bacteria were employed as models here, the D_2O-Raman method is generally applicable to a much wider range of cells. For example, a database of MIC-MA and MIC-MA-HI can be built to assess and compare metabolic-activity inhibitory effects of presently available antibiotics on the frequently encountered pathogens and cosmopolitan microbes. This database is complementary to the MIC-based one[43], and can serve as a new guideline to physicians in recommending the optimal type, dose and duration of antibiotics. As demonstrated in the case of ampicillin here, MIC-MA based recommendations of treatment regimen can be very different from

those derived from MIC, thus the MIC-MA derived guideline might be valuable not just for patient treatment but for the combat against spread of antibiotic resistance. Moreover, the D_2O-Raman method may form the basis of a new drug screening platform, as it can potentially measure drug effect on metabolism of mammalian or human cells at single-cell resolution. Furthermore, the independence of cell propagation is a highly desirable feature of the method that can be exploited for personalized drug sensitivity testing. In summary, the D_2O-Raman method and the MIC-MA and MIC-MA-HI concepts can serve as a generally applicable technological foundation for quantitative efficacy evaluation of antimicrobials, selection of drug treatment regimens and personalized drug sensitivity assessment and precision medicine.

Supporting Information

Supporting Information Available: Method description of the microorganisms and growth conditions used, Acquisition of Single-cell Raman Spectra, Tests for Minimal Inhibitory Concentration of selected antimicrobial drugs, and Measurements of intracellular ATP content from bulk cells; Supplemental tables for MIC measurements and statistical analysis; Supplemental figures for change of OD_{600}, Single-cell Raman spectra, C-D ratio or inter-cellular heterogeneity in metabolic activity with time or drug dose. This material is available free of charge via the Internet at http://pubs.acs.org.

Acknowledgements

J.X. acknowledges support of grants 91231205, 31327001 and 31425002 from NSFC and XDB15040100 from CAS. Y.J. acknowledges support of 2015ZDJS04002 from Shandong Province. Y.W thanks financial support of 31400436 from NSFC. W.E.H thanks support from EPSRC (EP/M002403/1) and NERC (NE/M002934/1) in the UK. S.H thanks support from NSFC (31400089) and China Postdoctoral Science Foundation Grant (2016LH00036). The authors thank Mingming Sun for the TOC artwork.

List of Abbreviations

CFU	Colony Forming Unit
CHX	chlorhexidine
MIC	Minimum Inhibitory Concentration

MIC-MA	Minimum Inhibitory Concentration based on Metabolic Activity
MIC-MA-HI	Heterogeneity Index of MIC-MA
NaF	sodium fluoride
NGMA	non-growing but metabolically active
SCRS	Single-cell Raman Spectra
SD	Standard Deviation

REFERENCES

1. Matthiessen, L.; Bergstrom, R.; Dustdar, S.; Meulien, P.; Draghia-Akli, R., *Lancet* **2016,** *388*, 865-865.
2. Laxminarayan, R.; Sridhar, D.; Blaser, M.; Wang, M. G.; Woolhouse, M., *Science* **2016,** *353*, 874-875.
3. Balouiri, M.; Sadiki, M.; Ibnsouda, S. K., *J Pharm Anal* **2016,** *6*, 71-79.
4. Bergkessel, M.; Basta, D. W.; Newman, D. K., *Nat Rev Microbiol* **2016,** *14*, 549-562.
5. Harms, A.; Maisonneuve, E.; Gerdes, K., *Science* **2016,** *354*.
6. Manina, G.; Dhar, N.; McKinney, J. D., *Cell Host Microbe* **2015,** *17*, 32-46.
7. Paloque, L.; Vidal, N.; Casanova, M.; Dumetre, A.; Verhaeghe, P.; Parzy, D.; Azas, N., *J Microbiol Meth* **2013,** *95*, 320-323.
8. Andreu, N.; Fletcher, T.; Krishnan, N.; Wiles, S.; Robertson, B. D., *J Antimicrob Chemother* **2012,** *67*, 404-414.
9. Hara, K. Y.; Shimodate, N.; Ito, M.; Baba, T.; Mori, H.; Mori, H., *Metab Eng* **2009,** *11*, 1-7.
10. Lobritz, M. A.; Belenky, P.; Porter, C. B. M.; Gutierrez, A.; Yang, J. H.; Schwarz, E. G.; Dwyer, D. J.; Khalil, A. S.; Collins, J. J., *Proc Natl Acad Sci* **2015,** *112*, 8173-8180.
11. Eldar, A.; Elowitz, M. B., *Nature* **2010,** *467*, 167-73.
12. Maglica, Z.; Ozdemir, E.; McKinney, J. D., *mBio* **2015,** *6*, e02236-14.
13. Assmann, C.; Kirchhoff, J.; Beleites, C.; Hey, J.; Kostudis, S.; Pfister, W.; Schlattmann, P.; Popp, J.; Neugebauer, U., *Anal Bioanal Chem* **2015,** *407*, 8343-52.
14. Schroder, U. C.; Beleites, C.; Assmann, C.; Glaser, U.; Hubner, U.; Pfister, W.; Fritzsche, W.; Popp, J.; Neugebauer, U., *Sci Rep-Uk* **2015,** *5*.
15. Teng, L.; Wang, X.; Wang, X.; Gou, H.; Ren, L.; Wang, T.; Wang, Y.; Ji, Y.; Huang, W. E.; Xu, J., *Sci Rep* **2016,** *6*, 34359.
16. Berry, D.; Mader, E.; Lee, T. K.; Woebken, D.; Wang, Y.; Zhu, D.; Palatinszky, M.; Schintimeister, A.; Schmid, M. C.; Hanson, B. T.; Shterzer, N.; Mizrahi, I.; Rauch, I.; Decker, T.; Bocklitz, T.; Popp, J.; Gibson, C. M.; Fowler, P. W.; Huang, W. E.; Wagner, M., *Proc Natl Acad Sci* **2015,** *112*, E194-E203.
17. Wang, Y.; Song, Y.; Tao, Y.; Muhamadali, H.; Goodacre, R.; Zhou, N. Y.; Preston, G. M.; Xu, J.; Huang, W. E., *Anal Chem* **2016,** *88*, 9443-9450.
18. Kumar, B. N. V.; Guo, S.; Bocklitz, T.; Rosch, P.; Popp, J., *Anal Chem* **2016,** *88*, 7574-82.
19. Eichorst, S. A.; Strasser, F.; Woyke, T.; Schintlmeister, A.; Wagner, M.; Woebken, D., *FEMS Microbiol Ecol* **2015,** *91*.
20. Van Loveren, C.; Spitz, L. M.; Buijs, J. F.; Ten Cate, J. M.; Eisenberg, A. D., *J Dent Res* **1991,** *70*, 1491-6.
21. Gross, E. L.; Leys, E. J.; Gasparovich, S. R.; Firestone, N. D.; Schwartzbaum, J. A.; Janies, D. A.; Asnani, K.; Griffen, A. L., *J Clin Microbiol* **2010,** *48*, 4121-4128.

22. Kostic, A. D.; Chun, E. Y.; Robertson, L.; Glickman, J. N.; Gallini, C. A.; Michaud, M.; Clancy, T. E.; Chung, D. C.; Lochhead, P.; Hold, G. L.; El-Omar, E. M.; Brenner, D.; Fuchs, C. S.; Meyerson, M.; Garrett, W. S., *Cell Host Microbe* **2013,** *14*, 207-215.
23. Rubinstein, M. R.; Wang, X. W.; Liu, W. D.; Hao, Y. J.; Cai, G. F.; Han, Y. P. W., *Cell Host Microbe* **2013,** *14*, 195-206.
24. Gao, S. G.; Li, S. G.; Ma, Z. K.; Liang, S.; Shan, T. Y.; Zhang, M. X.; Zhu, X. J.; Zhang, P. F.; Liu, G.; Zhou, F. Y.; Yuan, X.; Jia, R. N.; Potempa, J.; Scott, D. A.; Lamont, R. J.; Wang, H. Z.; Feng, X. S., *Infect Agents Cancer* **2016,** *11*.
25. Abranches, J.; Lemos, J. A.; Burne, R. A., *Fems Microbiol Lett* **2006,** *255*, 240-6.
26. Loesche, W. J., *Microbiol Rev* **1986,** *50*, 353-380.
27. Mak, P. A.; Rao, S. P. S.; Tan, M. P.; Lin, X. H.; Chyba, J.; Tay, J.; Ng, S. H.; Tan, B. H.; Cherian, J.; Duraiswamy, J.; Bifani, P.; Lim, V.; Lee, B. H.; Ma, N. L.; Beer, D.; Thayalan, P.; Kuhen, K.; Chatterjee, A.; Supek, F.; Glynne, R.; Zheng, J.; Boshoff, H. I.; Barry, C. E.; Dick, T.; Pethe, K.; Camacho, L. R., *ACS Chem Biol* **2012,** *7*, 1190-1197.
28. Sutton, S. V. W.; Bender, G. R.; Marquis, R. E., *Infect Immun* **1987,** *55*, 2597-2603.
29. Cheung, H. Y.; Wong, M. M. K.; Cheung, S. H.; Liang, L. Y.; Lam, Y. W.; Chiu, S. K., *PLoS One* **2012,** *7*.
30. Wise, E. M.; Park, J. T., *Proc Natl Acad Sci* **1965,** *54*, 75-&.
31. Tipper, D. J.; Strominger, J. L., *Proc Natl Acad Sci* **1965,** *54*, 1133-1141.
32. Moore, B. A.; Jevons, S.; Brammer, K. W., *Antimicrob Agents Chemother* **1979,** *15*, 831-833.
33. Balaban, N. Q.; Merrin, J.; Chait, R.; Kowalik, L.; Leibler, S., *Science* **2004,** *305*, 1622-1625.
34. Sanchez-Romero, M. A.; Casadesus, J., *Proc Natl Acad Sci U S A* **2014,** *111*, 355-60.
35. Bowen, W. H., *J R Soc Med* **1995,** *88*, 505-7.
36. Liao, Y.; Chen, J.; Brandt, B. W.; Zhu, Y.; Li, J.; van Loveren, C.; Deng, D. M., *PLoS One* **2015,** *10*, e0122630.
37. Wang, Y.; Ji, Y. T.; Wharfe, E. S.; Meadows, R. S.; March, P.; Goodacre, R.; Xu, J.; Huang, W. E., *Anal Chem* **2013,** *85*, 10697-10701.
38. Ji, Y.; He, Y.; Cui, Y.; Wang, T.; Wang, Y.; Li, Y.; Huang, W. E.; Xu, J., *Biotechnol. J* **2014,** *9*, 1512-8.
39. Zhang, P.; Ren, L.; Zhang, X.; Shan, Y.; Wang, Y.; Ji, Y.; Yin, H.; Huang, W. E.; Xu, J.; Ma, B., *Anal Chem* **2015,** *87*, 2282-9.
40. Zhang, Q.; Zhang, P.; Gou, H.; Mou, C.; Huang, W. E.; Yang, M.; Xu, J.; Ma, B., *The Analyst* **2015,** *140*, 6163-74.
41. Wang, T.; Ji, Y.; Wang, Y.; Jia, J.; Li, J.; Huang, S.; Han, D.; Hu, Q.; Huang, W. E.; Xu, J., *Biotech Biofuels* **2014,** *7*, 58.
42. Song Y, Davison PA, Frentrup M, Preston GM, Thompson IP, Murrell JC, Yin H, et al., *Microb Biotechnol*. 201610, 125-137.
43. Clinical and Laboratory Standards Institute. Performance standards for antimicrobial susceptibility testing; twenty-third informational supplement. CLSI document M100-S23CLSI, Wayne, PA, 2013.

Table

Table 1. Comparison between MIC-MA and MIC of three antibacterials for *Streptococcus mutans* UA159.

	NaF (g/L)	CHX (mg/L)	Ampicillin (mg/L)
MIC	0.4	2	0.8
MIC-MA	1.2	4	>50

Figures

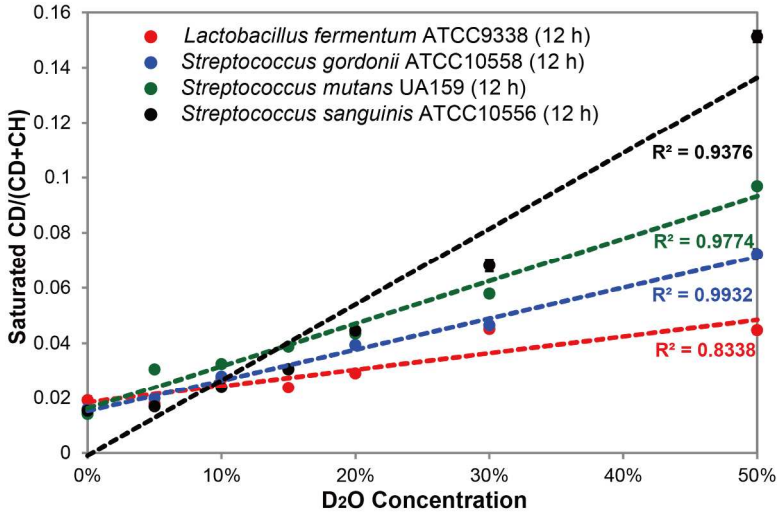

Figure 1. Correlation between the saturated C-D ratio and the D_2O concentration for four oral bacterial species. The bacteria were grown respectively under a series of D_2O levels and then cultured for 12 hours (when each culture reached the stationary phase and the C-D ratio also reached saturation), followed by SCRS measurement. Each point represents the average C-D ratio of SCRS from 60 cells (20 from each of three biological replicates of culture), with error bar indicating standard deviation among the three biological replicates.

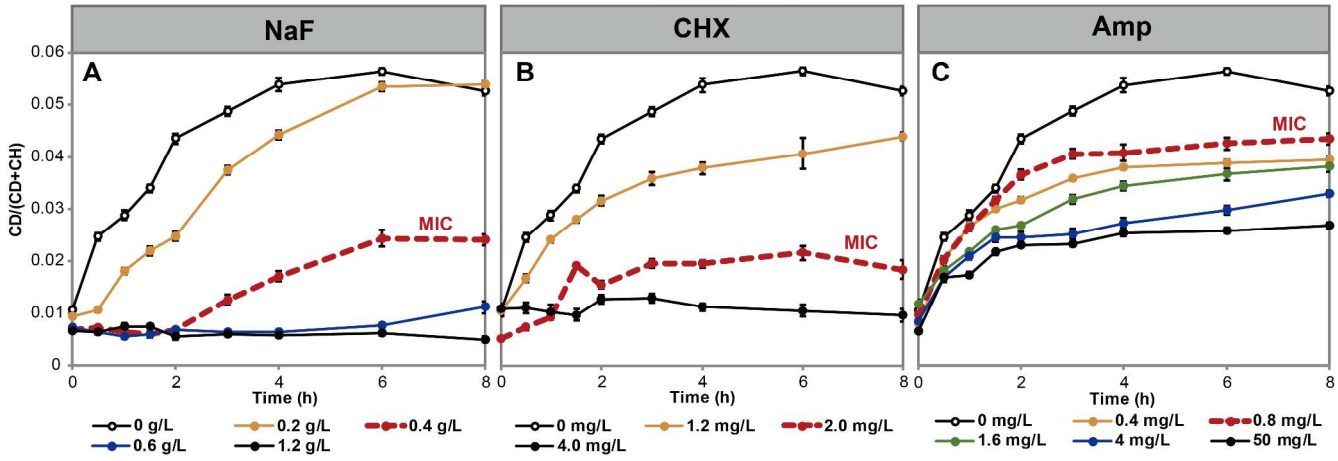

Figure 2. Temporal dynamics of the C-D ratio of *S. mutans* UA159 under increasing doses of NaF (A), CHX (B) or ampicillin (C). Each point represents the average C-D ratio of SCRS of 60 cells (20 from each of three biological replicates of culture), with error bar indicating standard deviation among the three biological replicates.

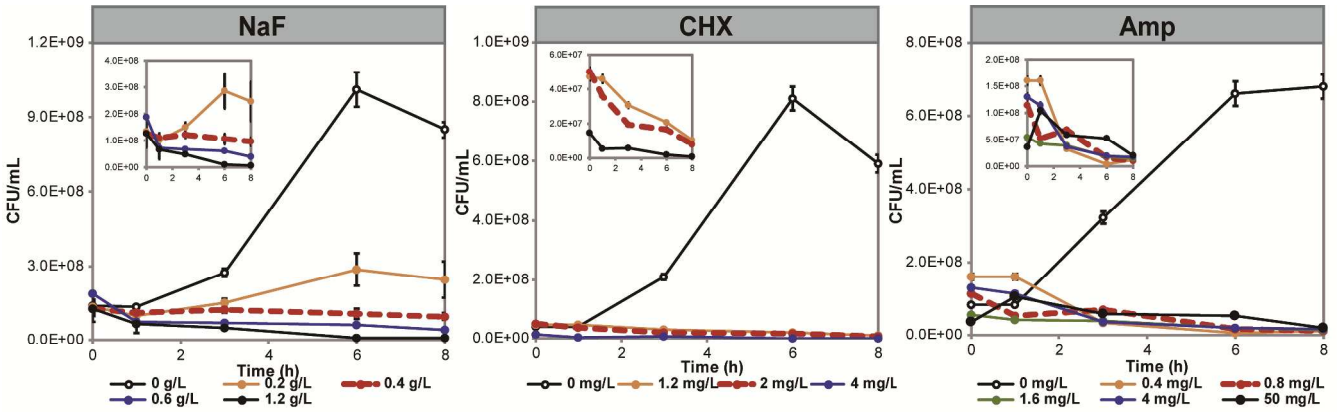

Figure 3. Cell recovery probability after various duration of treatment under a series of drug doses. Cells from cultures under drug treatments were collected at each time point, washed to remove residual medium, diluted with fresh BHI medium for a series of times, plated onto BHI agar and cultured at 37 ℃ for 36 h. Those plates with Colony forming units (CFUs) between 30 to 300 were counted. Value represents calculated CFU in 1 mL culture and error bar indicates standard error. For clear view of the cell recovery rates after drug treatment, CFU curves with drug-free controls masked were shown as insets.

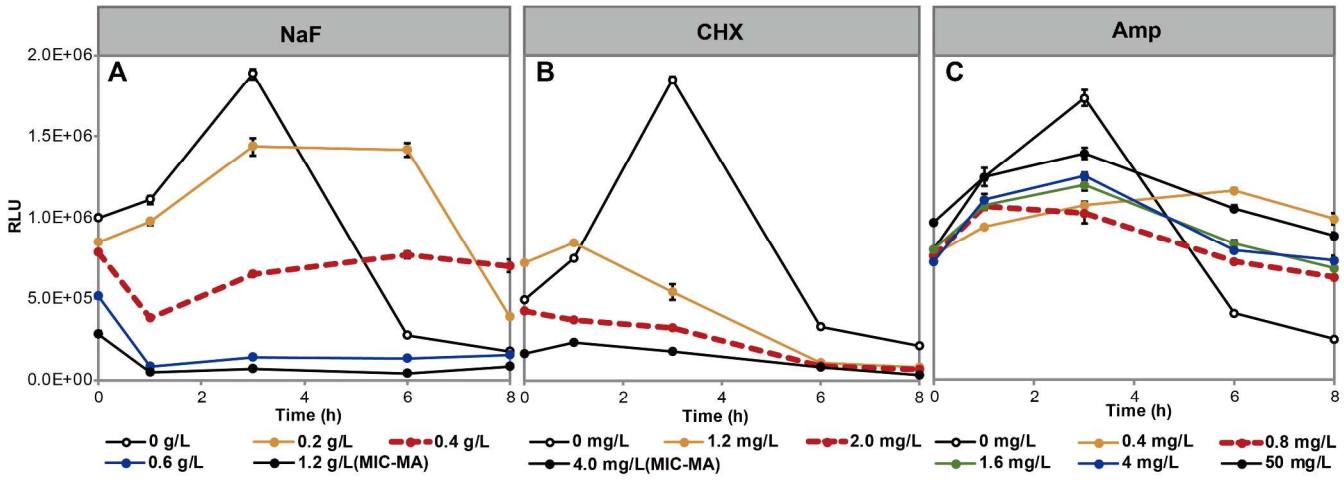

Figure 4. Temporal dynamics of the intracellular ATP level of bulk *S. mutans* UA159 cells under increasing doses of NaF (A), CHX (B) or ampicillin (C). Cells were cultured in BHI broth under the drug doses in presence of 30% D_2O. Results are presented by means ± SE (n = 3).

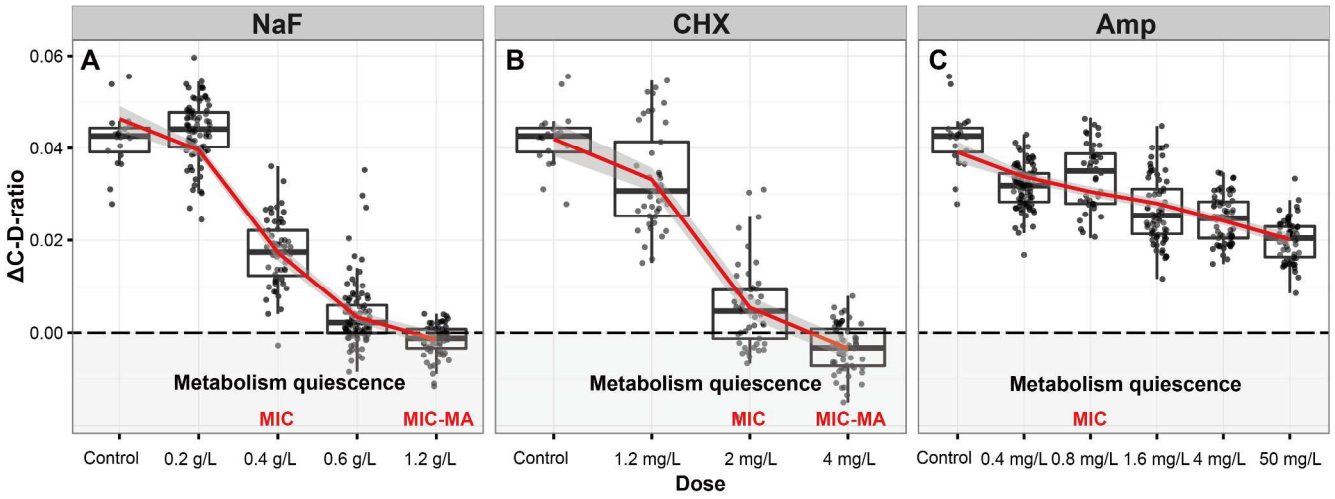

Figure 5. Dose effects of NaF (A), CHX (B) or ampicillin (C) on ΔC-D-ratio of *S. mutans* UA159 cells. ΔC-D-ratio at 8 h was plotted over the various doses. The red line, which was generated via the 'Loess' regression[43], represents the tendency of ΔC-D-ratio variation among the increasing doses. Each dot represents a cell.

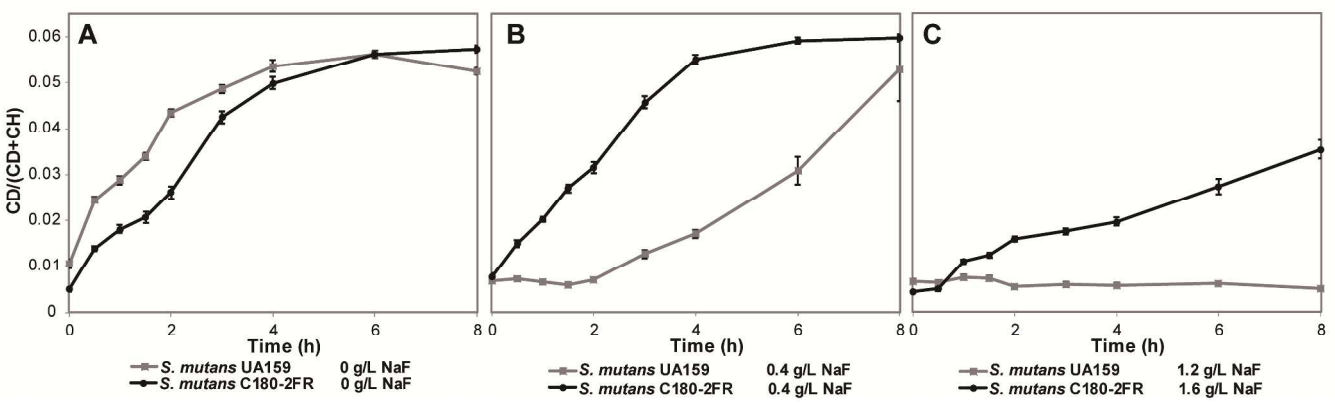

Figure 6. Temporal dynamics of C-D ratio for the NaF-sensitive *S. mutans* UA159 and the NaF-resistant C180-2FR cells under various doses of NaF. (**A**) NaF-free conditions on both strains. (**B**) 0.4 g/L NaF (MIC of UA159) for both strains. (**C**) 1.2 g/L NaF for UA159 and 1.6 g/L NaF (MIC of C180-2FR) for C180-2FR. Value represents the average C-D ratio of SCRS from 60 cells from three biological replicates, with error bar indicating standard error among 60 cells.

TOC: Measurement of MIC-MA using D_2O-Raman.